Earth and Planetary Science Letters 431 (2015) 15–25

Contents lists available at ScienceDirect

Earth and Planetary Science Letters

www.elsevier.com/locate/epsl

Identification of the static backstop and its influence on the evolution of the accretionary prism in the Nankai Trough

Takeshi Tsuji [a,b,*], Juichiro Ashi [c], Michael Strasser [d,e], Gaku Kimura [f]

[a] International Institute for Carbon-Neutral Energy Research (WPI-I2CNER), Kyushu University, Fukuoka, Japan
[b] Faculty of Engineering, Kyushu University, Fukuoka, Japan
[c] Atmosphere and Ocean Research Institute, the University of Tokyo, Tokyo, Japan
[d] Geological Institute, ETH Zurich, Zurich, Switzerland
[e] Institute of Geology, University of Innsbruck, Innsbruck, Austria
[f] Department of Earth and Planetary Science, the University of Tokyo, Tokyo, Japan

ARTICLE INFO

Article history:
Received 14 May 2015
Received in revised form 6 September 2015
Accepted 8 September 2015
Available online 22 September 2015
Editor: P. Shearer

Keywords:
backstop
accretionary prism evolution
forearc basin
fault system
Nankai trough
seismic profiles

ABSTRACT

To reveal the origin of a backstop and its influence on the evolution of the accretionary prism, we analyzed reflection seismic data acquired in the Nankai Trough off the Kii Peninsula. The deformation features of the forearc basin sequence show that the landward accretionary prism close to the coast was not deformed after the development of the forearc basin about 2–4 Ma. The surface of the landward prism can be identified as strong amplitude reflector, indicating that the landward prism has higher seismic velocity. Therefore, the landward accretionary prism inferred to be of higher strength constitutes a static backstop. Based on seismic and geologic observations, we interpret that the backstop was generated due to the large age differences of accreted material resulting from an inferred hiatus in subduction between ~13 and 6 Ma. The time-dependent processes such as the igneous activity in middle Miocene further contribute to the development of the backstop. A ridge structure beneath the forearc basin located trenchward of this backstop and running roughly parallel to it appears to reflect activity on an ancient splay fault. The strike of the ancient splay fault runs parallel to the backstop identified in this study and oblique to the current trench. This geometry suggests that location and mechanical behavior of this splay fault system is influenced by the backstop, and its distribution could be related to the coseismic rupture area.

1. Introduction

Geologic structures and dynamics of young accretionary prisms in convergent margins have been well characterized using seismic and drilling data (e.g., Shipley et al., 1994; Gulick et al., 2011; Moore et al., 2009; Kimura et al., 1997, 2011; Park and Kodaira, 2012; Strasser et al., 2009; Ramirez et al., 2015; Yamada et al., 2013). However, older accretionary prisms on the landward side of these bodies have not been well characterized, because their internal structure cannot be clearly imaged on seismic reflection profiles. Therefore, the process by which young accretionary prisms are preserved and in places converted into lithified crust is poorly known. The relationship between old and young accretionary prisms is important for efforts to integrate outcrop observations on land with seismic observations in offshore accretionary prisms (e.g., Hashimoto et al., 2013; Rowe et al., 2009).

The backstop, defined as a tectonic structure that has significantly greater strength than the sedimentary sequence lying trenchward of it (Silver et al., 1985; Byrne et al., 1993; Kopp and Kukowski, 2003), must strongly influence the accretion process and earthquake rupture process, but in most convergent margins its position has not been determined. Indeed, it is difficult to directly measure the strength of the accretionary prism. Lithification, the crucial mechanical change affecting sediments in an accretionary prism, may create the backstop (i.e., a mechanical boundary) against which younger sediments are accreted (Byrne and Hibbard, 1987). The backstop also partitions subducting material, either directing it into the accretionary prism or diverting it deeper into the subduction zone (Bangs et al., 2003). Because the backstop controls the shape of the accretionary prism, characterizing it is important for understanding deformation within the prism (e.g., fault distribution) as well as evolution of the forearc basin

* Corresponding author at: International Institute for Carbon-Neutral Energy Research (WPI-I2CNER), Kyushu University, Fukuoka, Japan. Tel.: +81 92 802 6875; fax: +81 92 802 6875.
E-mail address: tsuji@i2cner.kyushu-u.ac.jp (T. Tsuji).

http://dx.doi.org/10.1016/j.epsl.2015.09.011

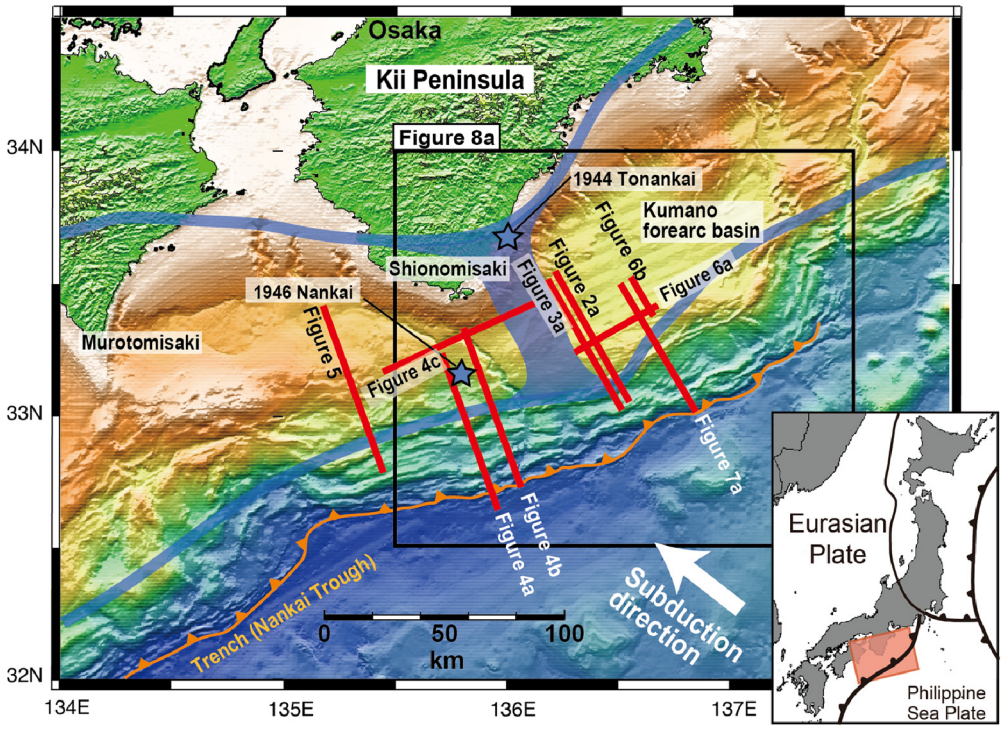

Fig. 1. Seafloor topography of the Nankai Trough region off the Kii Peninsula. The red lines indicate the seismic profiles shown in this study. Blue stars are the hypocenters of the 1944 Tonankai and the 1946 Nankai earthquakes. The blue boundaries indicate the segmentations of these interplate earthquakes. (For interpretation of the references to color in this figure, the reader is referred to the web version of this article.)

(Silver et al., 1985; Kopp and Kukowski, 2003). Many modeling studies have focused on how backstop geometry affects subduction processes (e.g., Byrne et al., 1993; Wang and Davis, 1996), but field seismic observations have been few (e.g., Trehu et al., 1994; Bangs et al., 2003). In non-accretionary convergent margins that undergo subduction erosion (e.g., Japan Trench), the edge of the continental crust often functions as the backstop (von Huene et al., 1994; Tsuru et al., 2002). In the Japan Trench, the location of this mechanical boundary is clearly identified from seafloor bathymetry and reflection profiles, and it may have played an important role in the coseismic rupture and tsunami generation of the 2011 Tohoku-oki earthquake (Tsuji et al., 2013a). In contrast, the origin of backstop in accretionary prisms (e.g., Nankai Trough, Barbados accretionary prism) and its influence on coseismic rupture distribution has not been well documented.

The accretionary prism is well developed in the Nankai Trough, where the Philippine Sea plate is subducting beneath southwest Japan (Fig. 1). Because this convergent margin repeatedly generates large interplate earthquakes (Ando, 1975), geophysical data were intensively acquired to characterize fault distribution. The recent drilling campaign along the Kumano transect has enabled us to determine the age of the sediments making up the accretionary prism as well as the forearc basin, which is useful information for characterizing the evolution of the accretionary prism (Kimura et al., 2011; Hayman et al., 2012; Moore et al., 2015). Therefore, this accretionary prism is a suitable field to study the origin and role of a backstop.

The speed and direction of plate subduction have dramatically changed in the Nankai Trough (Kimura et al., 2005, 2014; Hayman et al., 2012), as it has at other convergent margins. Kimura et al. (2014) interpreted that the plate subduction has paused and restarted in the Nankai Trough. Discontinuities in the subduction process might generate lithologic discontinuities within the accretionary prism, and the stiffer material of an older accretionary prism might establish a backstop. In this study, we used several seismic reflection profiles and drilling data acquired in the Nankai accretionary prism off Cape Shionomisaki, Japan, to identify the backstop and analyze the evolution history of the accretionary prism. Seismic properties of the accretionary prism and Kumano forearc basin enabled us to identify the backstop and infer its influence on the accretionary prism including fault system.

2. Seismic data

We used multichannel seismic reflection data acquired by several 2D surveys and a 3D survey (Figs. 2–7). Our main source was 2D seismic data acquired during cruise ODKM of R/V *Polar Princess* in 2003, which employed a tuned airgun array with a total volume of ~70 L fired at 50 m intervals and a streamer 6 km long with 480 receivers. This seismic data was acquired in a dense orthogonal geometry in the Nankai accretionary prism off Kumano, and its survey lines extend close to the coast of the Kii peninsula (Figs. 2, 3, and 6a). We also used data from other multichannel seismic reflection surveys conducted by R/V *Kairei* of JAMSTEC (Figs. 4 and 5; Park and Kodaira, 2012; Tsuji et al., 2013b, 2014b). These surveys employed an airgun array of ~200 L volume fired at 50 m intervals and a streamer ~5 km long with 204 receivers. Data processing for the 2D seismic data involved filtering, velocity analysis, stacking, deconvolution, and post-stack migration. To extract horizons of top surface of the accretionary prism from intersecting seismic reflection lines, we did not apply depth conversion to the time-domain seismic profiles. Indeed, the paucity of reflectors within the older accretionary prism prevented us from estimating seismic velocities for a depth conversion.

We also used a 3D seismic reflection survey acquired by M/V *Nordic Explorer* (Moore et al., 2009) to characterize the detailed geological structure of the accretionary prism (Figs. 6b and 7). The 12 × 56 km survey area included the Kumano forearc basin (Fig. 8a). We applied 3D prestack depth migration to the 3D seismic data using a tomography-based approach to obtain the high-

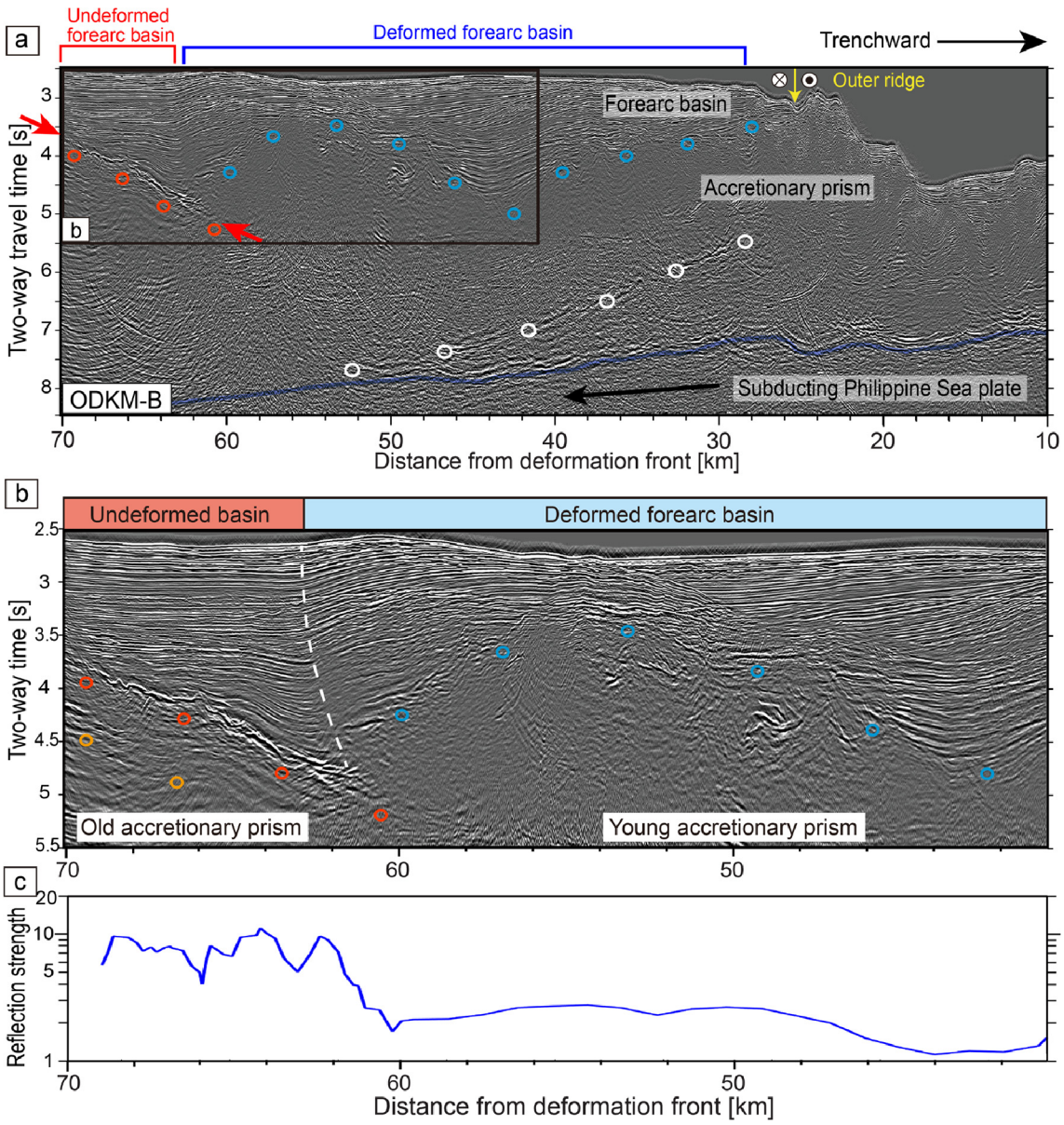

Fig. 2. Seismic profiles off Kumano (east of Cape Shionomisaki) showing the HA-LF reflector (red arrows). (a) Seismic profile for trench-normal direction at locations given in Fig. 1 (Tsuji et al., 2014b) and (b) its enlarged profile. Red and blue dots show the top of the old and young accretionary prism, respectively. Orange dots show the reflection parallel to the HA-LF reflector. White dots indicate the detachment of the present splay fault at the outer ridge (i.e., dynamic backstop). Blue line is the top of the subducting oceanic crust. (c) Reflection amplitude of the top of the accretionary prism displayed in panel (b). (For interpretation of the references to color in this figure, the reader is referred to the web version of this article.)

resolution P-wave velocity distribution within the forearc basin (Fig. 7b).

3. Results and interpretations

3.1. Location of the backstop

On the seismic profiles, we found clear differences in deformation features of the forearc basin sedimentary sequences near the east coast of the Kii Peninsula (cf. deformed vs. undeformed sediment sequences above red and blue dots, respectively, as shown in Figs. 2 and 3). Most of the sequence above the landward part of the accretionary prism is not deformed and shows horizontally-stratified reflection pattern. This indicates that the landward (older) accretionary prism beneath the undeformed forearc basin has not been deformed since the sedimentation of forearc basin began at ~2–4 Ma (Expedition 319 Scientists, 2010; Ramirez et al., 2015; Moore et al., 2015). On the other hand, the sequence above the trenchward (younger) prism is very deformed and reflections are tilted landward (Fig. 2b) (e.g., Gulick et al., 2010). This change in deformation style of the forearc basin sequences suggests that the mechanical properties (e.g., strength) of the underlying accretionary prism also change across the boundary between the landward prism beneath the undeformed forearc basin and trenchward prism beneath the deformed basin.

At the top of the landward accretionary prism beneath the undeformed forearc basin, a strong reflection is apparent on seismic profile (red dots in Figs. 2 and 3). The amplitude (or reflection coefficient) of the strong reflection is ~3.5 times greater than that of the trenchward younger prism surface (Fig. 2c), indicating that the seismic velocity beneath the strong reflector is significantly higher than that of trenchward prism. By considering the acoustic impedance of the Kumano basin sediment and accretionary prism,

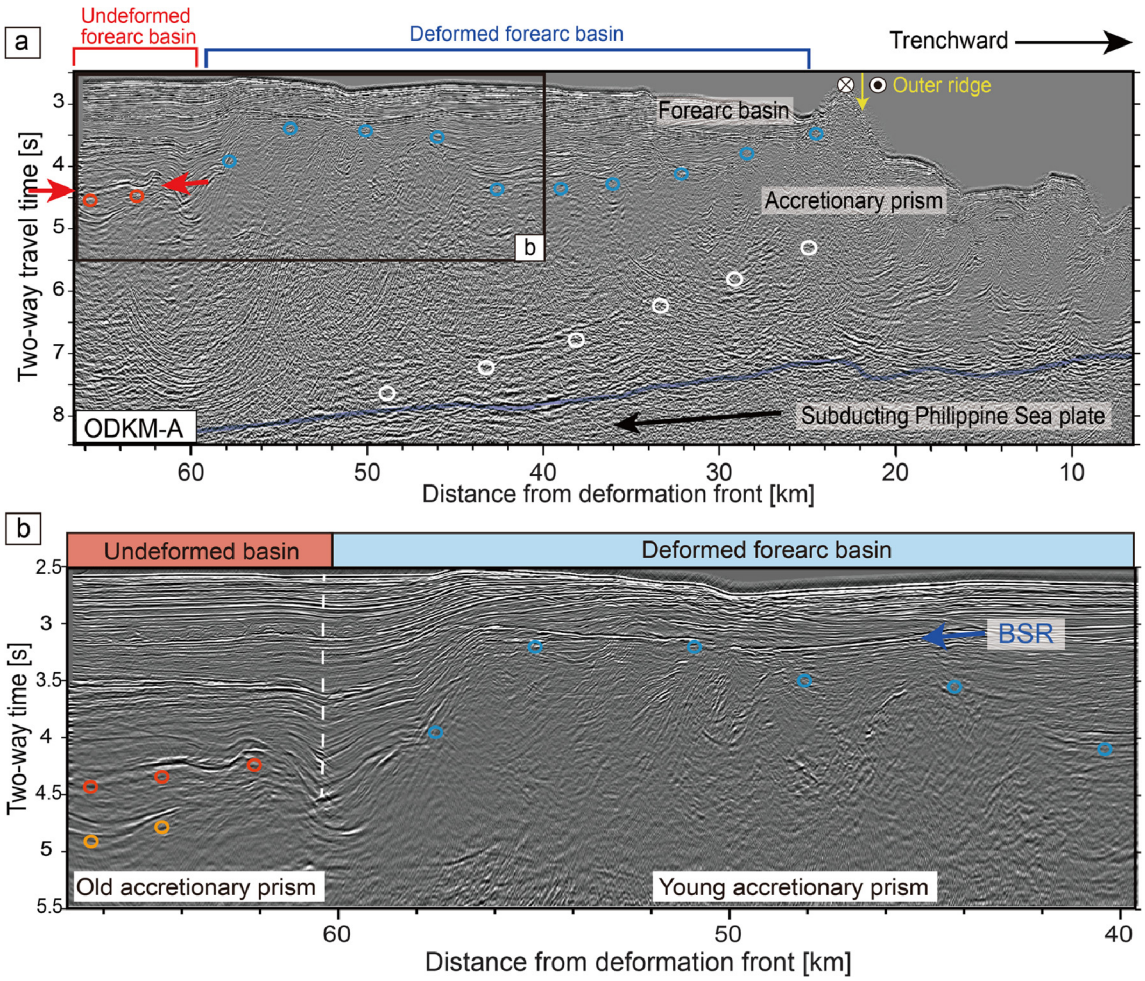

Fig. 3. Seismic profiles off Kumano (east of Cape Shionomisaki) showing the HA-LF reflector (red arrows). (a) Seismic profile for trench-normal direction at locations given in Fig. 1 and (b) its enlarged profile. Red and blue dots show the top of the old and young accretionary prism, respectively. Orange dots show the reflection parallel to the HA-LF reflector. White dots indicate the detachment of the present splay fault at the outer ridge (i.e., dynamic backstop). Blue line is the top of the subducting oceanic crust. (For interpretation of the references to color in this figure, the reader is referred to the web version of this article.)

we estimated the P-wave velocity beneath the high-amplitude reflector as ~3800 m/s and its density as ~2.4 g/cm^3. In this calculation, we assumed that the P-wave velocity of the Kumano basin sediment is 2000 m/s and that of the trenchward accretionary prism is 2500 m/s, and the density of both materials is 2.0 g/cm^3, all on the basis of logging data and vertical seismic profiling data obtained at Integrated Ocean Drilling Program (IODP) Site C0009 (Expedition 319 Scientists, 2010; Tsuji et al., 2011). Even though this estimate of P-wave velocity and density is based on several assumptions and thus contains uncertainties, the estimated P-wave velocity (~3800 m/s) is much higher than that of typical sedimentary rock in the Nankai accretionary prism (2000–3000 m/s; Kamei et al., 2012). The dominance in low-frequency of the strong reflection (Figs. 2 and 3) further indicates a significant velocity increase from forearc basin to accretionary prism (Costain and Çoruh, 2004). Therefore, the accretionary prism beneath the high-amplitude, low-frequency (HA-LF) reflector must be much more consolidated than the trenchward younger prism.

These findings indicate that the landward older prism beneath the undeformed forearc basin (or beneath the HA-LF reflector) constitutes a backstop (Fig. 9). The Kumano forearc basin sediment just trenchward of the proposed backstop is still deformed due to prism thickening, therefore the backstop could be still working and influencing the accretionary prism evolution and mechanical behavior. Observations using all available seismic profiles further indicate that the backstop extends parallel to the eastern coastline of the Kii Peninsula (red lines in Fig. 8a). Therefore, the distance from the trench to the backstop varies along a trench-parallel direction.

The backstop we identified in this study is interpreted as a static backstop, which is a fixed backstop with high strength (Kopp and Kukowski, 2003). The static backstop casts a stress shadow over the area, allowing the presence of a less-deformed forearc basin (Byrne et al., 1993; Kopp and Kukowski, 2003). The dynamic backstop, which is a trenchward mechanical boundary controlling dynamic deformation during coseismic rupture (Wang and Hu, 2006), is located at the outer ridge area (~30 km trenchward of the static backstop beneath the Kumano forearc basin; Fig. 2). In the outer ridge area, well-developed fractures associated with reverse or strike-slip faults (Tsuji et al., 2014b; Martin et al., 2010) decouple the trenchward and landward prisms.

3.2. Origin of the backstop

Gabbroic rock is observed at Cape Shionomisaki that has been dated to approximately 15–13 Ma (Hoshi et al., 2003). An igneous dome is clearly observed on the seismic profiles from off Cape Shionomisaki as defined by similar HA-LF reflection (red dots in Fig. 4; profile location in Figs. 1 and 8a) (Tsuji et al., 2013b). Because the location of the HA-LF reflector at Cape Shionomisaki coincides with a gravity anomaly and high seismic velocity area

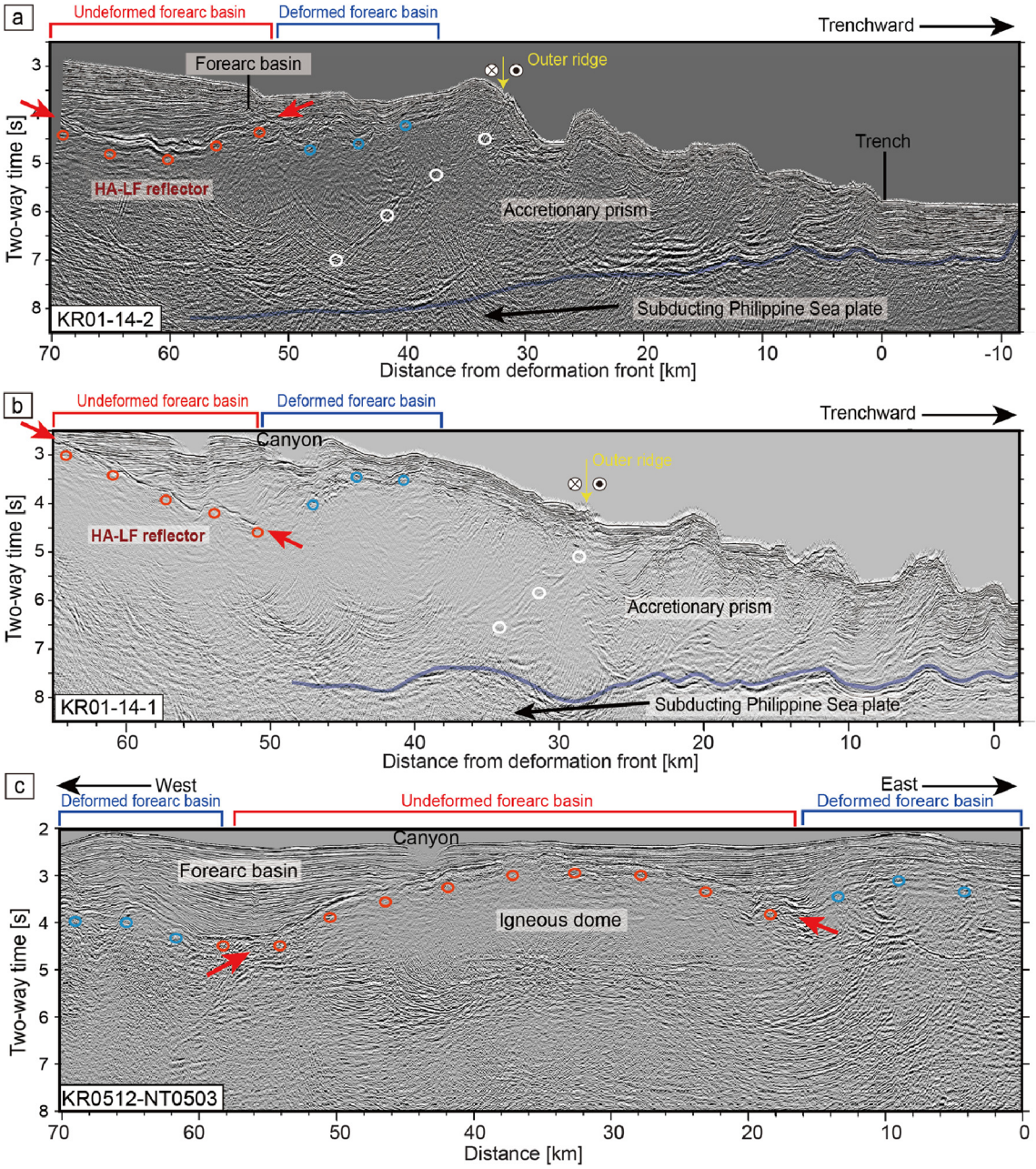

Fig. 4. Seismic profiles off Cape Shionomisaki showing an inferred igneous dome (red arrows). (a) and (b) Seismic profiles for trench-normal direction (Park and Kodaira, 2012; Tsuji et al., 2014b) and (c) its trench-parallel profile (Tsuji et al., 2013b) at locations given in Fig. 1. Red and blue dots show the top of the igneous dome and young accretionary prism, respectively. White dots indicate the present splay fault at the outer ridge (i.e., dynamic backstop). Blue line is the top of the subducting oceanic crust. (For interpretation of the references to color in this figure, the reader is referred to the web version of this article.)

(Kodaira et al., 2006; Kimura et al., 2014), that reflector could be interpreted as the surface of the igneous dome with high density. Since the thick accretionary prism is developed on its trenchward side of the igneous dome (Tsuji et al., 2013b), the igneous dome could also work as static backstop (i.e., igneous backstop). To the north of Cape Shionomisaki, furthermore, a ring dike several tens of kilometers across surrounds igneous rock, suggesting the presence of a caldera (Kawakami et al., 2007; Miura, 1999; Kimura et al., 2014; Fig. 8a). The gravity anomaly suggests that the igneous dome continues to the onland gabbroic rock at Cape Shionomisaki (Figs. 4 and 5 in Kimura et al., 2014). Therefore, the igneous body could be continuously distributed in NE–SW direction beneath the east coast of the Kii peninsula (Fig. 9). The stiff material influences the geometry and properties of the trenchward accretionary prism.

However, the HA-LF reflector beneath the Kumano forearc basin area (red dots in Figs. 2 and 3) is not associated with a gravity anomaly, and therefore the igneous dome is not expected in this region. The high-density layer beneath the Kumano forearc basin should be thin. The seismic profiles show the reflector at ~0.5 s (~500 m) deeper than the HA-LF reflector (orange dots in Figs. 2 and 3), suggesting the layered structure at the backstop surface. We interpreted the HA-LF reflector beneath the Kumano basin as representing volcaniclastic rocks deposited over the accretionary prism from the volcanic activity (15–13 Ma) in the Kii Peninsula (e.g., lithified deposits from pyroclastic flows of Trofimovs et al., 2006; Fig. 9a). Indeed, the pyroclastic unit of ~14 Ma was observed immediately overlying the basaltic crust at the Nankai Trough off Muroto, west of our survey area (Pickering et al., 1993). If the HA-LF reflector represents such volcanic-sedimentary

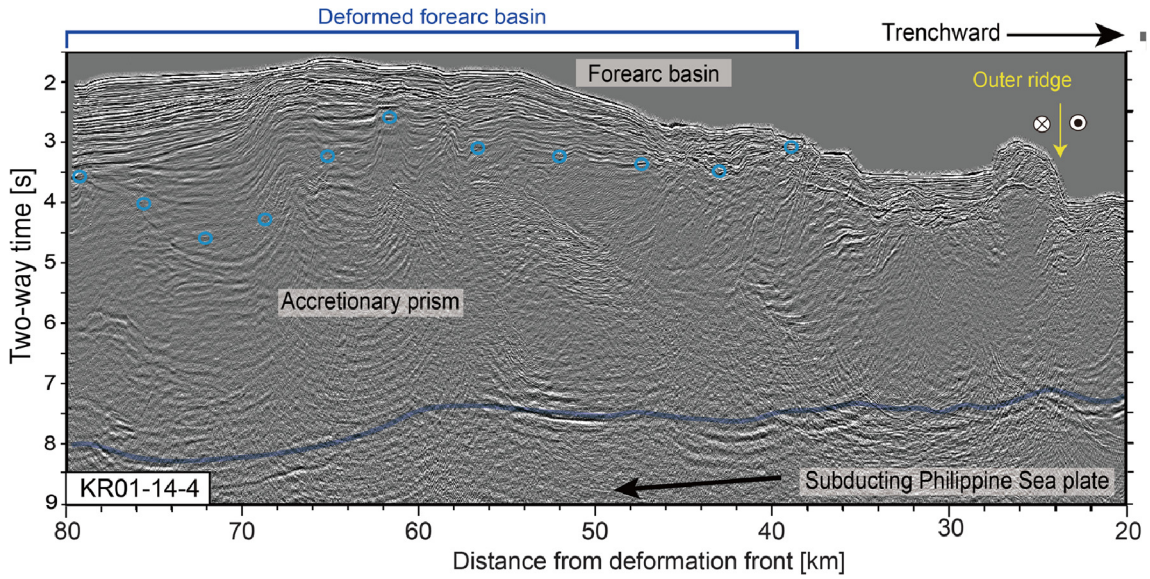

Fig. 5. Seismic profile west of Cape Shionomisaki. The profile location is given in Fig. 1. Blue dots show the top of the young accretionary prism. Blue line is the top of the subducting oceanic crust. (For interpretation of the references to color in this figure, the reader is referred to the web version of this article.)

rocks associated with the igneous rock emplacement and related volcanic activity, the accretionary prism beneath the HA-LF reflector was in place before the emplacement of igneous rock at 15–13 Ma (e.g., Kimura et al., 2005; Sumii and Shinjoe, 2003; Iwano et al., 2007). Whereas, the age of sediments comprising the uppermost accretionary prism at Site C0009, ~20 km closer to the trench than the HA-LF reflector (Fig. 8a), was estimated to ~6 Ma (Expedition 319 Scientists, 2010). This age gap in the accretionary prism indicates that the accretion process was halted from 13 Ma to ~6 Ma (Fig. 9). This interpretation agrees well with the triple junction migration hypothesis of Kimura et al. (2014) which also postulated cessation of subduction during this time period. Because Site C0009 is ~20 km trenchward from the edge of the HA-LF reflector, there is a possibility that the accretion restarted a little earlier than 6 Ma. However, it is difficult to accurately estimate the age of accretion process from the sedimentation age. Therefore, the age discussed here (Fig. 9) could include error but they are estimated to be smaller than 1 Ma.

The age gap between the two prisms accounts for the difference in their strength, with the older prism (possibly altered by the igneous intrusions) being stiffer. Since the older prism is directly covered by sediment of the Kumano forearc basin (~2–4 Ma; Figs. 2 and 3), the HA-LF reflector must have been exposed at the surface, without relatively little sedimentation taken place until the sedimentation of the forearc sequence began (from 13 to 4 Ma; Fig. 9a). Alternatively, a thicker, previously deposited sedimentary sequence deposited above the HA-LF reflector could also have been eroded during a later stage of the hiatus represented by the age gap between the HF-LA reflector and forarc-basin sedimentation.

As alternative interpretations, the HA-LF reflector beneath the Kumano basin may represent cemented sandstone or an erosional surface on the old prism, which also would result in high seismic velocities and generate a strong reflector. Indeed the old prism close to the igneous intrusions is rapidly consolidated (or lithified) due to the thermal diagenesis and has higher strength. The drilling in the Costa Rica convergent margin found that a strong reflector at the top of the accretionary prism corresponds to cemented coarse sandstone (Kimura et al., 1997). In any of these interpretations, the landward prism beneath the HA-LF reflector should be much older than the trenchward prism and should function as a backstop. No other significant velocity variation is observed within the accretionary prism in the study area (Kamei et al., 2012). Therefore, it appears that consolidation has not been significant trenchward of the backstop, and that the backstop interface identified here is the largest mechanical boundary associated to lithification in this region.

3.3. Geometry of the backstop

The trenchward edge of the HA-LF reflector is unclear within the accretionary prism on seismic profiles (Figs. 2 and 3), and it is difficult to tell whether its dip is trenchward or landward. The dip direction has a strong influence on the development of an accretionary prism (Byrne et al., 1993). The growth structure of the forearc basin sediment above the accretionary prism on the seaward side of the HA-LF reflector (Fig. 2b) indicates progressive slip on the surface of the backstop interface. Therefore, the backstop interface in our study area might be trenchward-dipping and propagate within the accretionary prism.

Byrne and Hibbard (1987) also proposed a trenchward-dipping backstop from observations of the Shimanto belt on the landward side of the Nankai accretionary prism, because the lithification front is thermally controlled. In this study, we propose that an age difference in the prism material resulting from a hiatus in subduction (Kimura et al., 2014) contributed to the construction of the backstop. The thermal gradient within the Miocene accretionary prism was very high in this region (Byrne and Hibbard, 1987); therefore, consolidation was strongly promoted in the old accretionary prism.

3.4. Influence of the backstop on prism evolution

A buried ridge beneath the Kumano forearc basin was locally extracted by Tsuji et al. (2014a) from 3D seismic volume (Figs. 6c, 8c). In this study, we extracted the buried ridge for a wide area beneath the Kumano forearc sediment using several 2D seismic profiles (Fig. 8b). The continuous buried ridge system extends in a NE–SW direction beneath the Kumano forearc basin. This ridge system is the most prominent feature of the top of the accretionary prism. At its southwest end, the ridge system appears to merge into the present outer ridge, although the ridge structure is unclear on seismic profiles due to recent fault activities around the outer ridge. The buried ridge structure is ~1 km high (Figs. 6 and 8c),

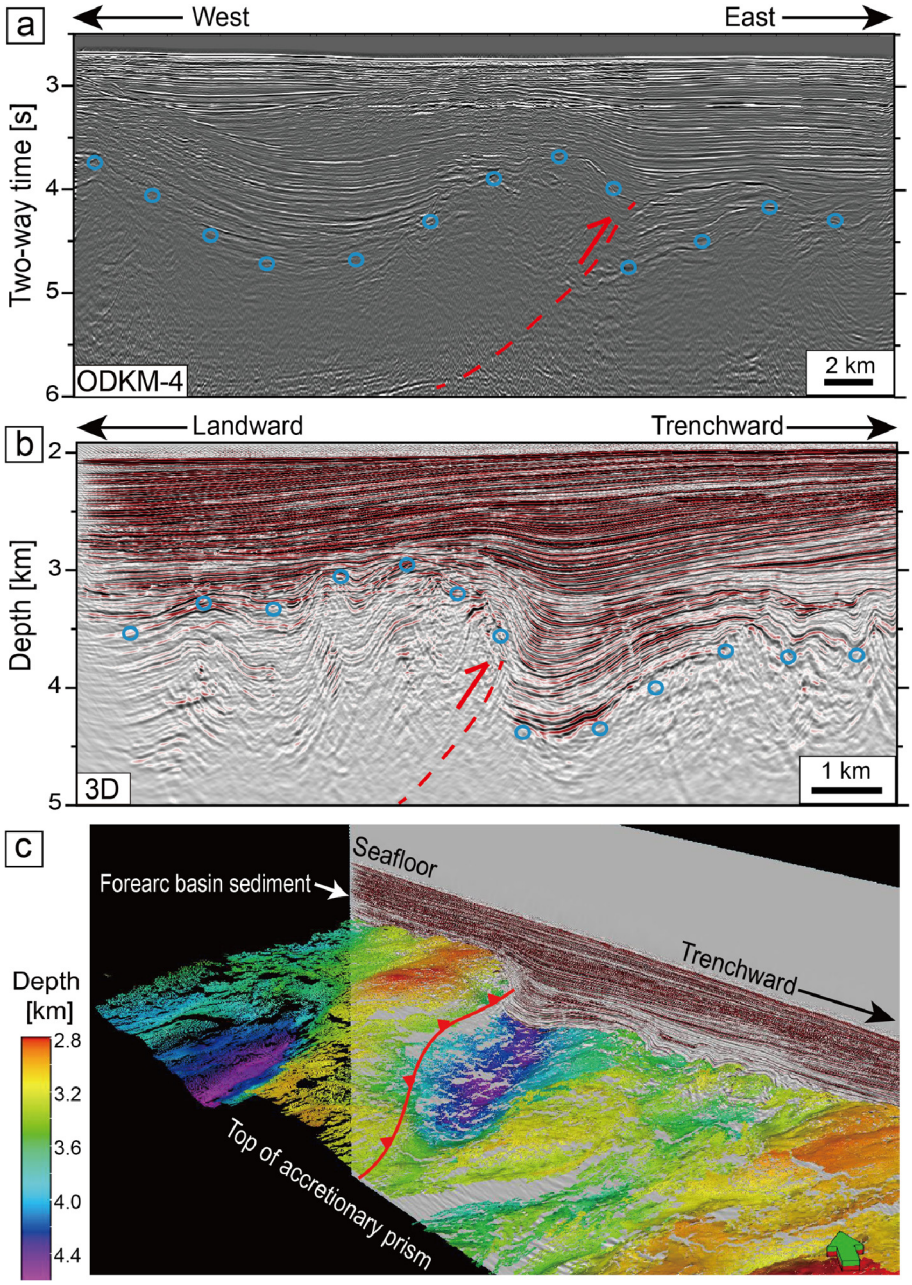

Fig. 6. Seismic profiles off Kumano (east of Cape Shionomisaki) showing the ridge system generated by ancient splay fault displacements. (a) Seismic profile for trench-parallel direction at locations given in Fig. 1. Blue dots indicate the top of young accretionary prism. Red dashed line shows the inferred ancient splay fault. (b) Seismic profile for trench-normal direction extracted from 3D seismic volume. (c) 3D geometry of the top of the accretionary prism extracted from 3D seismic volume. Red line indicates the trace of the interpreted ancient fault. (For interpretation of the references to color in this figure, the reader is referred to the web version of this article.)

nearly the same height as the present outer ridge off the Kii Peninsula. A belt of abnormal pore pressure observed beneath the ridge structure soles into the detachment (Fig. 7a; Tsuji et al., 2014a). A prominent landward-dipping reflector can be observed on the reflection profiles (red dashed line in Fig. 6). The offset by reverse displacement at the trace of the interpreted fault was identified on the seismic profiles (Fig. 6; Ramirez et al., 2015). Therefore, we interpreted that the buried ridge was generated as the result of activity on an ancient prominent out-of-sequence thrust (likely splay fault). The mapped orientation of the ridge indicates that the strike of the ancient fault was much different from that of the present splay fault beneath the fore-arc high. Since the seismic profiles show the deformation of forearc basin sequences above the ancient fault, this fault system could be still active after the sedimentation of forearc basin. However, since the offset (ridge height) due to the thrust displacement is much larger than the deformation of the forearc basin sequence (Fig. 6), we interpreted that the ancient thrust was originated before the sedimentation of forearc basin. Recently, Ramirez et al. (2015) showed that the thrust movements initiated in the outer wedge area (trenchward of the outer ridge), based on detailed analysis of the forearc basin sequence.

The seismic data (Fig. 7b) shows a low-amplitude and low-velocity zone above the ancient splay fault (or buried ridge system), indicating that overpressured fluid is moving upward along the interpreted ancient splay fault. Overpressure derived from fluid flow on the ancient splay fault is compatible with the presence of the mud volcanoes developed along the northern extension of the ridge system (red arrows in Fig. 8a). Indeed, Nishio et al. (2015) demonstrated that pore fluid in one of these mud volcanoes is de-

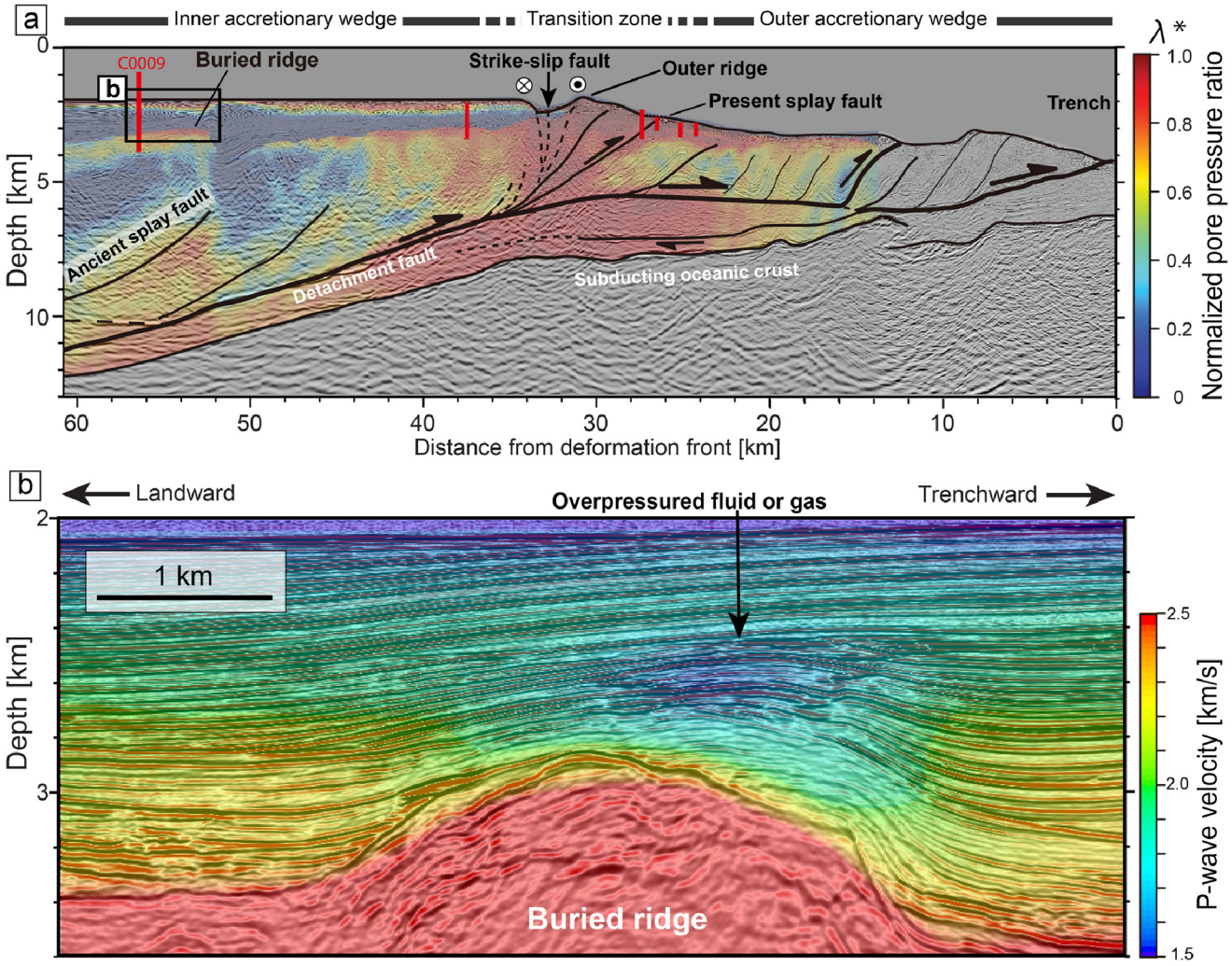

Fig. 7. Seismic profile off Kumano (east of Cape Shionomisaki) showing inferred structures and pore pressures. (a) Fault system and pore pressure distribution (Tsuji et al., 2014a) at location given in Fig. 1. This profile shows the inferred ancient splay fault (~53 km from deformation front). Color indicates the normalized pore pressure ratio predicted from seismic velocity. (b) P-wave velocity predicted by the 3D tomography inversion during prestack depth migration. The overpressured zone, which may be the source of mud volcanism, is identified as a low-amplitude and low-velocity zone in the forearc basin sequence. (For interpretation of the colors in this figure, the reader is referred to the web version of this article.)

rived from a deep (~15 km) seismogenic fault. The aligned mud volcanoes demonstrate that the buried ridge system could continue to the northern side of the Kumano forearc basin beneath the mud volcano chain and the deep-sourced fluids further corroborate our interpretation of this fault system to be a splay fault system. These features appear to have developed parallel to the edge of backstop as well as the coastline of the Kii Peninsula (Fig. 8).

The presence of an ancient splay fault parallel to the backstop interface suggests that the backstop strongly controlled the structure within the accretionary prism. By this reasoning, the trench axis formed immediately after subduction has resumed at ~6 Ma also would have run parallel to the coastline (NE–SW) (Fig. 9b). Since the subduction direction of the Philippian Sea plate at 6 Ma would be almost similar to the present direction (e.g., Ide et al., 2010), the trench axis was normal to the subduction direction when subduction was restarted (Fig. 9), and the splay fault would have behaved as a pure reverse fault. Later, after repeated subduction of ridge structures aligned with the present trench axis (e.g., the paleo-Zenisu ridge in Fig. 8a; Park et al., 2003), the trench axis moved outboard from the Eurasia plate in the eastern part of the Kumano region (Fig. 9c). As a result, the trench as well as present splay fault is oblique to the plate subduction direction, and the present splay fault could be dominance in strike-slip motion (Tsuji et al., 2014b). In addition, a slight change in plate subduction direction after 6Ma (~15 degree) inferred from core observations of IODP sites (Hayman et al., 2012) may also influence the fault motion.

3.5. Influence of the backstop on earthquake rupture segment

Since the backstop influences fault systems in accretionary prisms (e.g., the ancient splay fault) linking to the plate interface, its distribution could relate to the segmentation of the earthquake rupture area. At the forearc basin off the west coast of the Kii peninsula, we could not identify a landward, undeformed forearc basin sequence, nor did we observe the HA-LF reflector (Fig. 5). Thus, the backstop is discontinuously distributed in trench parallel direction, and it is projected to be closest to the trench just offshore the Cape Shionomisaki (Fig. 8a).

The segment boundary between the 1944 Tonankai earthquake (Mw8.1) and the 1946 Nankai earthquake (Mw8.4) is located at the southwestern edge of the backstop (Kodaira et al., 2006), where the igneous backstop edge is close to the trench axis (Fig. 8a). Because of the discontinuous backstop off the Cape Shionomisaki, the characteristics of fault systems, including the plate interface,

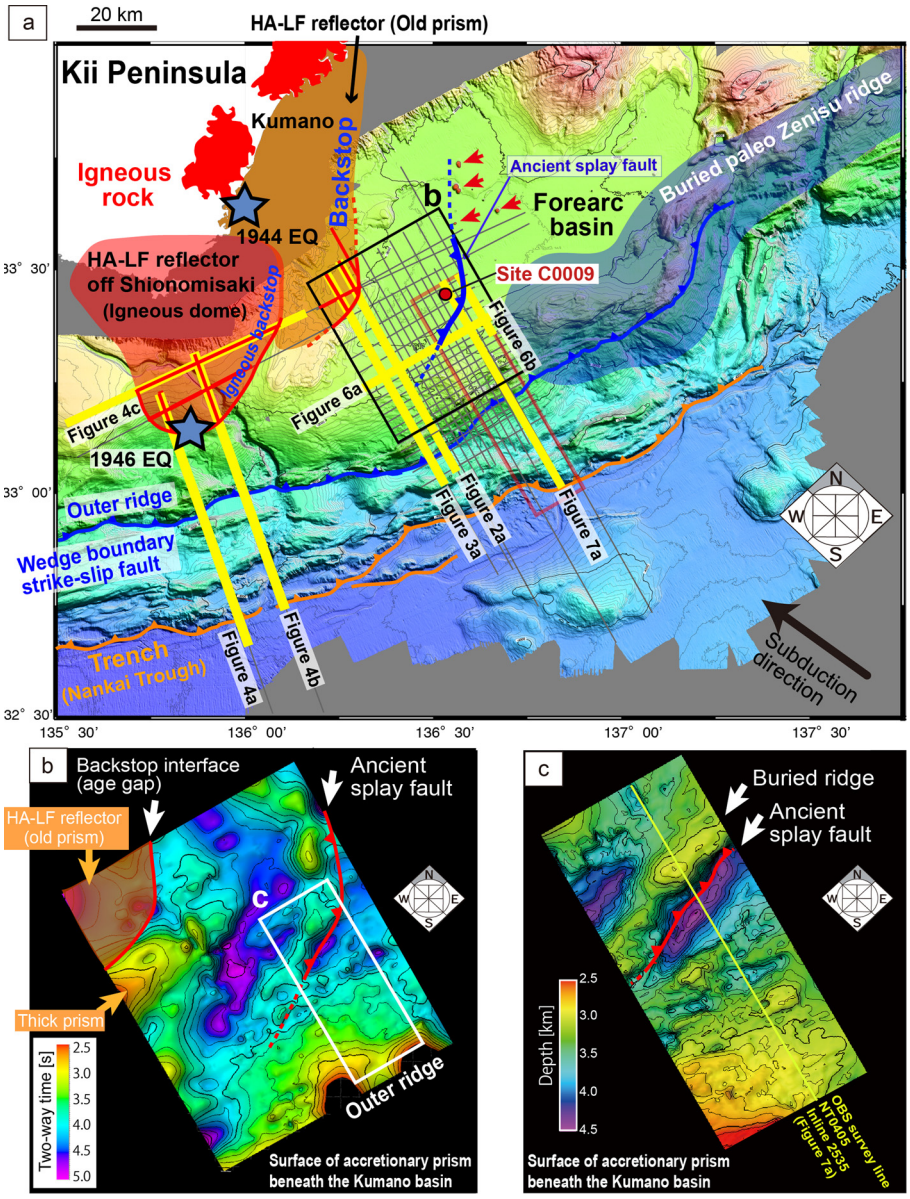

Fig. 8. Seafloor and surface of the accretionary prism off Kumano (east of Cape Shionomisaki). (a) Detailed seafloor topography of the study area. The HA-LF reflector beneath the undeformed forearc basin (orange-shaded zone) and igneous dome (red-shaded zone) are identified on the seismic profiles (intervals indicated by red lines). Thin black lines indicate seismic profiles we used in this study. The blue shaded area shows the recently subducted paleo-Zenisu ridge (Park et al., 2003). Blue lines show the currently active splay fault and the ancient splay fault. Red arrows are mud volcanoes along the northern continuation of the ancient splay fault. Blue stars indicate the hypocenters of the 1944 Tonankai and the 1946 Nankai earthquakes. (b) The top of accretionary prism buried beneath the Kumano forearc basin, extracted from several 2D seismic lines. The color indicates two-way travel time. Red line indicates the ancient splay fault. The orange-shaded zone shows the HA-LF reflector. (c) Detail of panel (b), showing depth to the top of the accretionary prism from Tsuji et al. (2014a). This geometry is extracted from 3D seismic data and same as Fig. 6c.

is discontinuous at the segment boundary. Previous studies have shown that around the Cape Shionomisaki, the subduction angle changes (Shiomi et al., 2008), and the Philippine Sea plate is split (Ide et al., 2010). Furthermore, the stress orientation changes at the Cape Shionomisaki (Mochizuki et al., 2010). These variations around the Cape Shionomisaki could be influenced by the discontinuous backstop identified in this study. Furthermore, the igneous backstop with high-density increases the overburden for the plate interface (Tsuji et al., 2013b). Therefore, the distribution of the backstop with high strength could relate to the boundary of coseismic rupture area, although other factors also control rupture characteristics (e.g., geometry of the subducting plate; Wang and Bilek, 2014). These implications are not solely related to the Nankai Trough, but much may apply to other plate convergent margins.

4. Conclusions

We identified the static backstop by focusing on the reflection characteristics of the forearc basin and accretionary prism in the Nankai Trough. The static backstop in the accretionary prism could be originated by a hiatus in subduction process. The igneous activity also contributes to the orientation of the backstop. As the subduction resumed at ~6 Ma, the trench axis would have run parallel to the backstop, as is the orientation of ancient splay fault system, which highlights that the backstop can influence the structures and evolution of the accretionary prism. Because the backstop controls the fault system and influences the properties of plate interface, its distribution could relate to the earthquake rupture segment. Indeed the segment boundary of interplate earthquakes is located at the southwestern edge of the backstop, where the backstop is close to the trench axis.

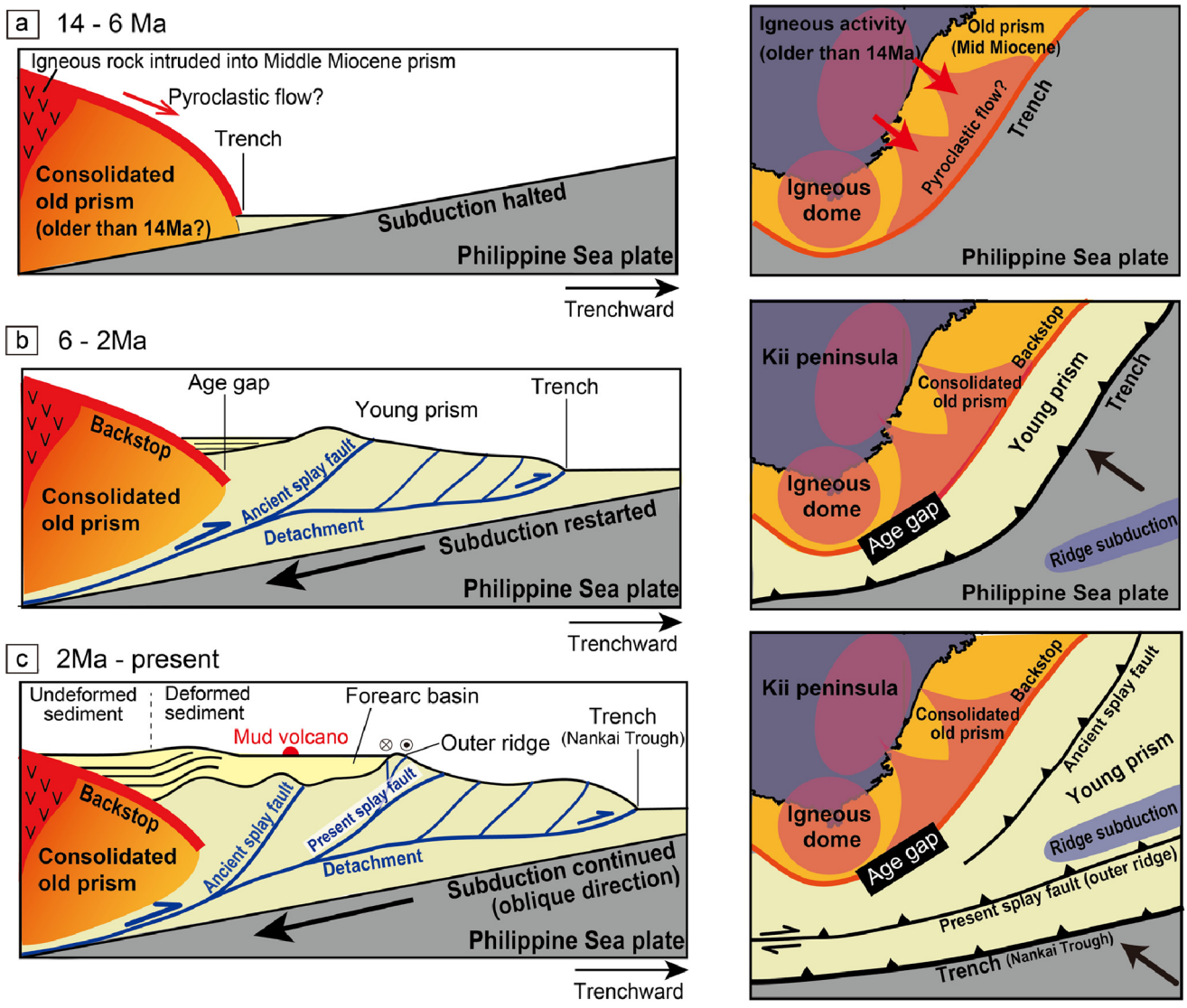

Fig. 9. Schematic diagrams showing the evolution of the accretionary prism off Kumano at (a) 14–6 Ma, (b) 6–2 Ma and (c) 2 Ma–present. Left panels are profiles extending from the coast to the trench; right panels show map views.

Acknowledgements

M. Conin and N. Hayman reviewed this manuscript and gave us constructive comments. We used 2D seismic reflection data acquired by JAMSTEC. The 3D seismic data were acquired with the support of the Ministry of Education, Culture, Sports, Science, and Technology (MEXT) and the U.S. National Science Foundation (NSF). This research was supported by the JSPS through a Grant-in-Aid for Science Research B (No. 15H02988), Grant-in-Aid for Scientific Research on Innovative Areas (No. 15H01143), and Grant-in-Aid for Scientific Research (S) (No. 15H05717). T. Tsuji gratefully acknowledges the support of the I2CNER, sponsored by the WPI, MEXT, Japan. M. Strasser acknowledges support by Swiss National Science Foundation (No. PP00P2-133481).

References

Ando, M., 1975. Source mechanisms and tectonic significance of historical earthquakes along the Nankai Trough. Tectonophysics 27, 119–140. http://dx.doi.org/10.1016/0040-1951(75)90102-X.

Bangs, N.L., Christeson, G.L., Shipley, T.H., 2003. Structure of the Lesser Antilles subduction zone backstop and its role in a large accretionary system. J. Geophys. Res. 108, 2358. http://dx.doi.org/10.1029/2002JB002040, B7.

Byrne, D.E., Hibbard, J., 1987. Landward vergence in accretionary prisms: the role of the backstop and thermal history. Geology 115, 1163–1167.

Byrne, D.E., Wang, W., Davis, D.M., 1993. Mechanical role of backstops in the growth of forearcs. Tectonics 12 (1), 123–144. http://dx.doi.org/10.1029/92TC00618.

Costain, J.K., Çoruh, C., 2004. Basic theory of exploration seismology with Mathematica notebooks and examples on CD-ROM. Handbook of Geophysical Exploration, Seismic Exploration 1, 195–252.

Expedition 319 Scientists, 2010. Site C0009 in NanTroSEIZE stage 2: NanTroSEIZE riser/riserless observatory. Proc. Integr. Ocean Drill. Program 319. http://dx.doi.org/10.2204/iodp.proc.319.103.2010.

Gulick, S.P.S., Bangs, N., Moore, G.F., Ashi, J., Martin, K.M., Sawyer, D.S., Tobin, H.J., Kuramoto, S., Taira, A., 2010. Rapid forearc basin uplift and megasplay fault development from 3D seismic images of Nankai Margin off Kii Peninsula, Japan. Earth Planet. Sci. Lett. 300, 55–62.

Gulick, S.P.S., Austin, J.A., McNeill, L.M., Bangs, N.L., Martin, K.M., Henstock, T.J., Bull, J.M., Dean, S.M., Djajadihardja, Y.S., Permana, H., 2011. Updip rupture of the 2004 Sumatra earthquake extended by thick indurated sediments. Nat. Geosci. 4, 453.

Hashimoto, Y., Doi, N., Tsuji, T., 2013. Difference in acoustic properties at seismogenic fault along a subduction interface: application to estimation of effective pressure and fluid pressure ratio. Tectonophysics 600, 134–141. http://dx.doi.org/10.1016/j.tecto.2013.03.016.

Hayman, N.W., Byrne, T.B., McNeill, L.C., Kanagawa, K., Kanamatsu, T., Browne, C.M., Schleicher, A.M., Huftile, G.J., 2012. Structural evolution of an inner accretionary wedge and forearc basin initiation, Nankai margin, Japan. Earth Planet. Sci. Lett. 353–354, 163–172.

Hoshi, H., Iwano, H., Danhara, T., Yoshida, T., 2003. Fission-track dating of the Shionomisaki igneous complex, Kii Peninsula, Japan. J. Geol. Soc. Jpn. 109 (3), 130–150.

Ide, S., Shiomi, K., Mochizuki, K., Tonegawa, T., Kimura, G., 2010. Split Philippine Sea Plate beneath Japan. Geophys. Res. Lett. 37, L21304. http://dx.doi.org/10.1029/2010GL044585.

Iwano, H., Danhara, T., Hoshi, H., Kawakami, Y., Sumii, T., Shinjoe, H., Wada, Y., 2007. Simultaneity and similarity of the Muro Pyroclastic flow deposit and the Kumano acidic rocks in Kii Peninsula, southwest Japan, based on fission track ages and morphological characteristics of zircon. J. Geol. Soc. Jpn. 113 (7), 326–339.

Kamei, R., Pratt, G., Tsuji, T., 2012. Waveform tomography imaging of a megasplay fault system in the seismogenic Nankai subduction zone. Earth Planet. Sci. Lett. 317–318, 343–353.

Kawakami, Y., Hoshi, H., Yamaguchi, Y., 2007. Mechanism of caldera collapse and resurgence: observations from the northern part of the Kumano acidic rocks, Kii peninsula, southwest Japan. J. Volcanol. Geotherm. Res. 167 (1), 263–281.

Kimura, G., Silver, E.A., Blum, P., et al., 1997. In: Proc. ODP. Initial Reports, vol. 170. http://dx.doi.org/10.2973/odp.proc.ir.170.1997. College Station, TX.

Kimura, J.-I., Stern, R.J., Yoshida, T., 2005. Reinitiation of subduction and magmatic responses in SW Japan during Neogene time. Geol. Soc. Am. Bull. 117 (7–8), 969–986.

Kimura, G., Moore, G.F., Strasser, M., Screaton, E., Curewitz, D., Streiff, C., Tobin, H., 2011. Spatial and temporal evolution of the megasplay fault in the Nankai Trough. Geochem. Geophys. Geosyst. 12, Q0A008. http://dx.doi.org/10.1029/2010GC003335.

Kimura, G., Hashimoto, Y., Kitamura, Y., Yamaguchi, A., Koge, H., 2014. Middle Miocene swift migration of the TTT triple junction and rapid crustal growth in southwest Japan: a review. Tectonics 33, 1219–1238. http://dx.doi.org/10.1002/2014TC003531.

Kodaira, S., Hori, T., Ito, A., Miura, S., Fujie, G., Park, J.-O., Baba, T., Sakaguchi, H., Kaneda, Y., 2006. A cause of rupture segmentation and synchronization in the Nankai trough revealed by seismic imaging and numerical simulation. J. Geophys. Res. 111, B09301. http://dx.doi.org/10.1029/2005JB004030.

Kopp, H., Kukowski, N., 2003. Backstop geometry and accretionary mechanics of the Sunda margin. Tectonics 22, 1072. http://dx.doi.org/10.1029/2002TC001420. 6 pp.

Martin, K.M., et al., 2010. Possible strain partitioning structure between the Kumano fore-arc basin and the slope of the Nankai Trough accretionary prism. Geochem. Geophys. Geosyst. 11, Q0AD02. http://dx.doi.org/10.1029/2009GC002668.

Miura, D., 1999. Arcuate pyroclastic conduits, ring faults, and coherent floor at Kumano caldera, southwest Honshu, Japan. J. Volcanol. Geotherm. Res. 92 (3), 271–294.

Mochizuki, K., Nakahigashi, K., Kuwano, A., Yamada, T., Shinohara, M., Sakai, S., Kanazawa, T., Uehira, K., Shimizu, H., 2010. Seismic characteristics around the fault segment boundary of historical great earthquakes along the Nankai Trough revealed by repeated long-term OBS observations. Geophys. Res. Lett. 37, L09304. http://dx.doi.org/10.1029/2010GL042935.

Moore, G., Park, J.-O., Bangs, N.L., Gulick, S.P., Tobin, H.J., Nakamura, Y., Sato, S., Tsuji, T., Yoro, T., Tanaka, H., Uraki, S., Kido, Y., Sanada, Y., Kuramoto, S., Taira, A., 2009. Structural and seismic stratigraphic framework of the NanTroSEIZE Stage 1 transectProc. In: IODP. http://dx.doi.org/10.2204/iodp.proc.314315316.102.2009. 314-315-316, College Station, TX (IODP Management International, Inc.).

Moore, G., Boston, B.B., Strasser, M., Underwood, M.B., Ratliff, R.A., 2015. Evolution of tectono-sedimentary systems in the Kumano Basin, Nankai Trough forearc. Mar. Pet. Geol. 67, 604–616.

Nishio, Y., Ijiri, A., Toki, T., Morono, Y., Tanimizu, M., Nagaishi, K., Inagaki, F., 2015. Origins of lithium in submarine mud volcano fluid in the Nankai accretionary wedge. Earth Planet. Sci. Lett. 414, 144–155. http://dx.doi.org/10.1016/j.epsl.2015.01.018.

Park, J.-O., Kodaira, S., 2012. Seismic reflection and bathymetric evidences for the Nankai earthquake rupture across a stable segment-boundary. Earth Planets Space 64, 299–303.

Park, J.-O., Moore, G.F., Tsuru, T., Kodaira, S., Kaneda, Y., 2003. A subducted oceanic ridge influencing the Nankai megathrust earthquake rupture. Earth Planet. Sci. Lett. 217, 77–88.

Pickering, K.T., Underwood, M.B., Taira, A., 1993. Stratigraphic synthesis of the DSDP-ODP sites in the Shikoku basin, Nankai Trough, and accretionary prism. In: Hill, I.A., Taira, A., Firth, J.V. (Eds.), Proc. ODP, Scientific Results, vol. 131, pp. 313–330. College Station, TX.

Ramirez, S.G., Gulick, S.P.S., Hayman, N.W., 2015. Early sedimentation and deformation in the Kumano forearc basin linked with Nankai accretionary prism evolution, southwest Japan. Geochem. Geophys. Geosyst. 16, 1616–1633. http://dx.doi.org/10.1002/2014GC005643.

Rowe, C.D., Meneghini, F., Moore, J.C., 2009. Fluid-rich damage zone of an ancient out-of-sequence thrust, Kodiak Islands, Alaska. Tectonics 28, TC1006. http://dx.doi.org/10.1029/2007TC002126.

Shiomi, K., Matsubara, M., Ito, Y., Obara, K., 2008. Simple relationship between seismic activity along Philippine Sea slab and geometry of oceanic Moho beneath southwest Japan. Geophys. J. Int. 173, 1018–1029.

Shipley, T.H., Moore, G.F., Bangs, N.L., Moore, J.C., Stoffa, P.L., 1994. Seismically inferred dilatancy distribution, northern Barbados Ridge decollement: implications for fluid migration and fault strength. Geology 22, 411–414.

Silver, E.A., Ellis, M.J., Breen, N.A., Shipley, T.H., 1985. Comments on the growth of accretionary wedge. Geology 13, 6–9.

Strasser, M., Moore, G.F., Kimura, G., Kitamura, Y., Kopf, A.J., Lallemant, S., Park, J.-O., Screaton, E.J., Su, X., Underwood, M.B., Zhao, X., 2009. Origin and evolution of a splay fault in the Nankai accretionary wedge. Nat. Geosci. 2, 648–652. http://dx.doi.org/10.1038/ngeo609.

Sumii, T., Shinjoe, H., 2003. K–Ar ages of the Ohmine Granitic Rocks, south-west Japan. Isl. Arc 12 (4), 335–347.

Tréhu, A.M., Asudeh, I., Brocher, T.M., Luetgert, J., Mooney, W.D., Nabelek, J.L., Nakamura, Y., 1994. Crustal architecture of the Cascadia forearc. Science 265, 237–243.

Trofimovs, J., et al., 2006. Submarine pyroclastic deposits formed at the Soufriere Hills volcano, Montserrat (1995–2003): what happens when pyroclastic flows enter the ocean? Geology 34, 549–552.

Tsuji, T., et al., 2011. In situ stress state from walkaround VSP anisotropy in the Kumano basin southeast of the Kii Peninsula, Japan. Geochem. Geophys. Geosyst. 12, Q0AD19. http://dx.doi.org/10.1029/2011GC003583.

Tsuji, T., Kawamura, K., Kanamatsu, T., Kasaya, T., Fujikura, K., Ito, Y., Tsuru, T., Kinoshita, M., 2013a. Extension of continental crust by anelastic deformation during the 2011 Tohoku-oki earthquake: the role of extensional faulting in the generation of a great tsunami. Earth Planet. Sci. Lett. 364, 44–58. http://dx.doi.org/10.1016/j.epsl.2012.12.038.

Tsuji, T., Kodaria, S., Ashi, J., Park, J.-O., 2013b. Widely distributed thrust and strike-slip faults within subducting oceanic crust in the Nankai Trough off the Kii Peninsula, Japan. Tectonophysics 600, 52–62. http://dx.doi.org/10.1016/j.tecto.2013.03.0142.

Tsuji, T., Kamei, R., Pratt, G., 2014a. Pore pressure distribution of a mega-splay fault system in the Nankai Trough subduction zone: insight into up-dip extent of the seismogenic zone. Earth Planet. Sci. Lett. 396, 165–178. http://dx.doi.org/10.1016/j.epsl.2014.04.011.

Tsuji, T., Ashi, J., Ikeda, Y., 2014b. Strike-slip motion of a mega-splay fault system in the Nankai oblique subduction zone. Earth Planets Space 66, 120. http://dx.doi.org/10.1186/1880-5981-66-120.

Tsuru, T., Park, J.-O., Miura, S., Kodaira, S., Kido, Y., Hayashi, T., 2002. Along-arc structural variation of the plate boundary at the Japan Trench margin: implication of interplate coupling. J. Geophys. Res. 107 (B12), 2357. http://dx.doi.org/10.1029/2001JB001664.

von Huene, R., Klaeschen, D., Cropp, B., 1994. Tectonic structure across the accretionary and erosional parts of the Japan Trench margin. J. Geophys. Res. 99, 22349–22361.

Wang, K., Bilek, S.L., 2014. Invited review paper: fault creep caused by subduction of rough seafloor relief. Tectonophysics 610, 1–24.

Wang, W.-H., Davis, D.M., 1996. Sandbox model simulation of forearc evolution and noncritical wedges. J. Geophys. Res. 101 (B5), 11329–11339. http://dx.doi.org/10.1029/96JB00101.

Wang, K., Hu, Y., 2006. Accretionary prism in subduction earthquake cycles: the theory of dynamic Coulomb wedge. J. Geophys. Res. 111, B06410. http://dx.doi.org/10.1029/2005JB004094.

Yamada, Y., Masui, R., Tsuji, T., 2013. Characteristics of a tsunamigenic megasplay fault in the Nankai Trough. Geophys. Res. Lett. 40, 4594–4598. http://dx.doi.org/10.1002/grl.50888.